

Thermal emittance measurements of a cesium potassium antimonide photocathode

Ivan Bazarov,^{a)} Luca Cultrera, Adam Bartnik, Bruce Dunham, Siddharth Karkare, Yulin Li, Xianghong Liu, Jared Maxson, and William Roussel
Cornell Laboratory for Accelerator-based Sciences and Education, Cornell University, Ithaca, New York 14853, USA

(Received 18 April 2011; accepted 11 May 2011; published online 2 June 2011)

Thermal emittance measurements of a CsK₂Sb photocathode at several laser wavelengths are presented. The emittance is obtained with a solenoid scan technique using a high voltage dc photoemission gun. The thermal emittance is 0.56 ± 0.03 mm mrad/mm(rms) at 532 nm wavelength. The results are compared with a simple photoemission model and found to be in a good agreement. © 2011 American Institute of Physics. [doi:10.1063/1.3596450]

Photocathodes play an increasingly important role in present and future accelerators requiring increasingly smaller emittance and higher current beams utilizing photoemission for electron generation. Not only high quantum efficiency (QE) but also small thermal (intrinsic) emittance and subpicosecond photoemission response are required. CsK₂Sb is well-known from streak camera applications and the photomultiplier tube industry to have prompt response and high QE in a convenient (visible) spectral range. However, thermal emittance, the other critical parameter for accelerators, has never been reported in the literature. We present such measurements obtained using a solenoid scan technique with a high voltage dc photoemission gun for CsK₂Sb excited with 532, 473, and 405 nm light. The results are compared with a simple theory and found in excellent agreement when using the values for band gap energy and electron affinity reported in the literature.

CsK₂Sb photocathodes are grown on heavily doped Si substrates in a dedicated chamber and subsequently translated into the high voltage dc gun¹ equipped with a load-lock system. Details of the photocathode preparation chamber and cathode recipe are available elsewhere.² Photocathodes with QE of 5%–7% in the green are routinely produced. Figure 1 shows QE versus the photon energy for the photocathode used in these measurements. Specific photon energies used in this experiment are indicated by the circles.

The experimental beamline used to measure thermal emittance is shown in Fig. 2. The relevant beamline elements are the dc gun, the solenoid, and the chemical vapor deposition diamond viewscreen positioned at 0.89 m from the photocathode. The solenoid current is varied and the beam size at the screen is recorded. The data are later fitted to obtain the emittance. The axial electric and magnetic fields are shown in Fig. 2 for 350 kV gun voltage and 4.2 A solenoid current. We employ dc lasers to deliver several microampere of beam current. The effects of the space charge are negligible as a result.

For the solenoid scan technique to work, it is critical to know the transfer matrices $\mathbf{R} = \mathbf{R}(i \rightarrow f)$, which relate the particle's transverse coordinate x and divergence dx/dz from before to after the region of interest

$$\begin{pmatrix} x \\ \frac{dx}{dz} \end{pmatrix}_f = \mathbf{R} \begin{pmatrix} x \\ \frac{dx}{dz} \end{pmatrix}_i \quad (1)$$

The use of a single solenoid implies coupling of x , y transverse planes, which requires more complicated treatment for beams with asymmetry and generally 4×4 size transfer matrices. Additionally, electric and magnetic fields overlap in a small region of our beamline and need to be properly accounted for. We found an efficient way to address this by obtaining an exact analytical solution for the 2×2 transfer matrix in the Larmor frame for the overlapping constant E , B fields (both along longitudinal or z direction) of length Δz

$$\mathbf{R}(\Delta z) = \begin{pmatrix} C & S \frac{\beta_i \gamma_i}{b} \\ -S \frac{b}{\beta_f \gamma_f} & C \frac{\beta_i \gamma_i}{\beta_f \gamma_f} \end{pmatrix} \quad (2)$$

Here, γ and β are Lorentz factors before (subscript i) and after (subscript f) the field region. $C \equiv \cos(\Delta\theta)$ and $S \equiv \sin(\Delta\theta)$ for Larmor angle $\Delta\theta \equiv \theta_f - \theta_i = (b/a) \ln[\gamma_f(1 + \beta_f)/\gamma_i(1 + \beta_i)]$. Normalized field strengths are $a \equiv eE/mc^2$

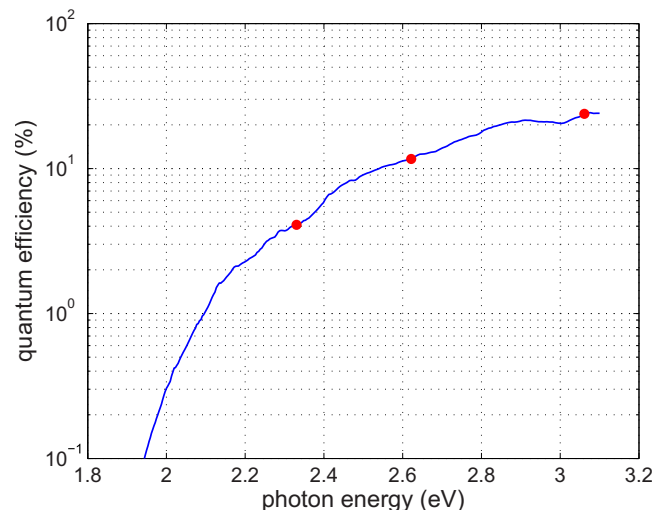


FIG. 1. (Color online) QE vs photon energy.

^{a)}Electronic mail: ib38@cornell.edu.

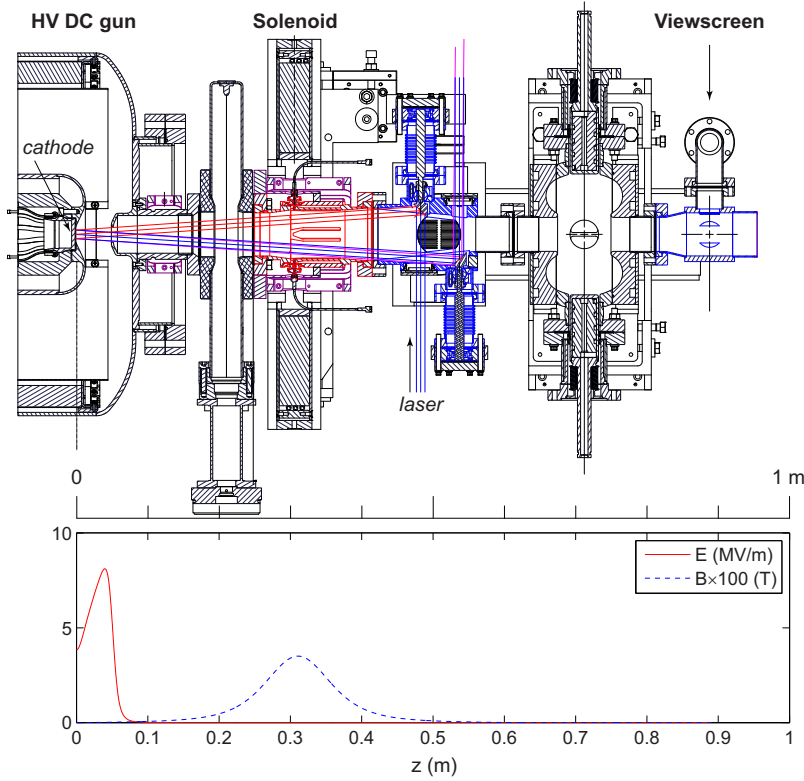


FIG. 2. (Color online) Experimental setup and fields.

and $b \equiv eB/2mc$. Lorentz factors before and after the field region are related by $\gamma_f = \gamma_i + a\Delta z$. The fundamental constants here are the electron mass m , charge e , and the speed of light c . The edge effect matrix (for rising and falling edges of E) is given by

$$\mathbf{R}_{\text{edge},i,f} = \begin{pmatrix} 1 & 0 \\ \mp \frac{a}{2\beta_{i,f}^2 \gamma_{i,f}} & 1 \end{pmatrix}. \quad (3)$$

The upper sign is taken with i subscript for the entrance (rising) edge $\mathbf{R}_{\text{edge},i}$, and the other choice for the exit (falling) edge. The full matrix from the cathode to the screen location (and the overall Larmor angle) is obtained by matrix multiplication of small Δz slices of $E(z)$ and $B(z)$ fields using $\mathbf{R}_{\text{edge},f} \mathbf{R}(\Delta z) \mathbf{R}_{\text{edge},i}$ for each individual interval (except right at the cathode, which does not include a rising E edge). Upon applying the counter-rotation to the screen image by the Larmor angle θ , the motion in x and y planes becomes decou-

pled and the solenoid scan analysis proceeds in a usual manner, e.g., see Ref. 3. The matrix formalism and the overall Larmor angle were verified both experimentally and through the particle tracking and were found to be in excellent agreement.

Upon rotation by the Larmor angle, each viewscreen image was processed⁴ to extract rms beam size in both planes. The rms beam size versus the solenoid current is used to determine the beam emittance, see Fig. 3 for an example of the solenoid scan fit. The emittance was measured at three different gun voltages: 110 kV, 230 kV, and 350 kV and was found to be the same within the uncertainty of the measurement. The 350 kV gun voltage corresponds to about 4 MV/m at the photocathode, which results in a Schottky correction to the work function of less than 0.1 eV.

The laser beam was 1:1 imaged onto the cathode after passing through a circular aperture. To account for possible photocathode QE variations and slight differences in laser delivery path to the gun, we use the results of the solenoid

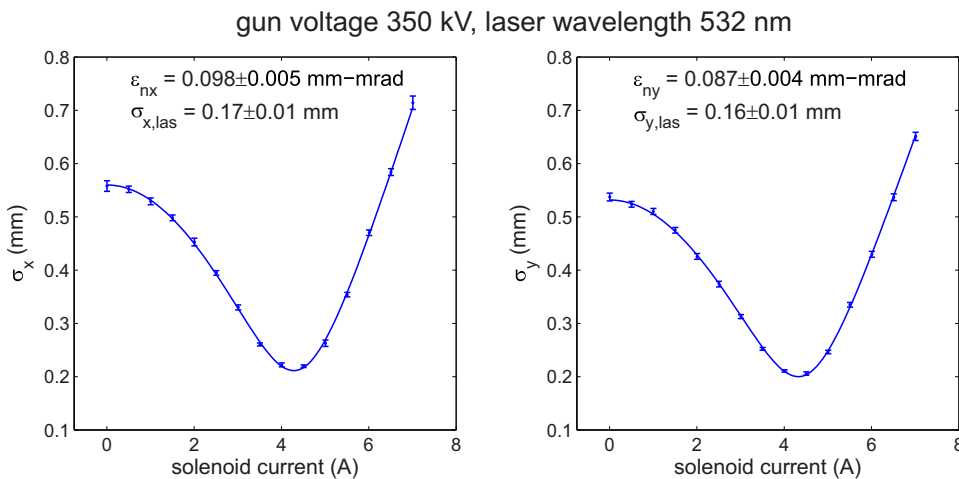


FIG. 3. (Color online) Solenoid scan and fit example.

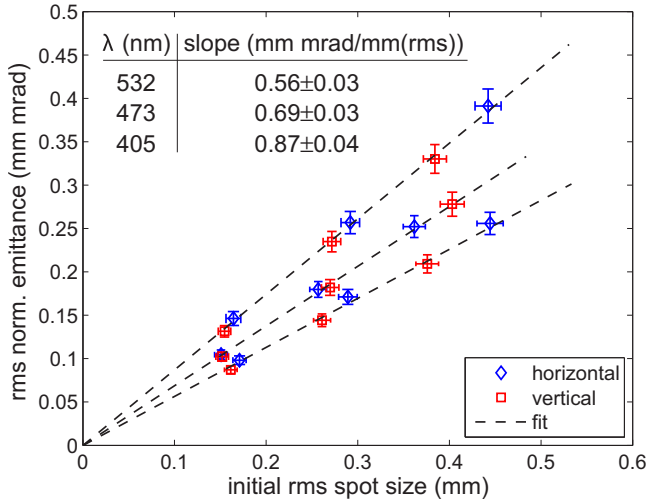


FIG. 4. (Color online) Thermal emittance for different wavelengths.

scan fit which returns the initial electron beam size at the location of the cathode in addition to the beam emittance. These values are in a good agreement with those obtained by measuring the laser image at a charge-coupled device camera positioned at the same distance from the imaging lens as the gun photocathode.

The summary of the results is shown in Fig. 4 for the three wavelengths (the gun voltage is 230 kV). The slope of normalized rms emittance with the rms laser spot size is indicated for each of the laser wavelengths.

Mean transverse energy (MTE) is often used as a figure of merit to characterize photocathode thermal emittance independent of the laser spot size. The rms normalized emittance at the cathode is given by

$$\epsilon_{nx} = \sigma_x \frac{\sqrt{\langle p_x^2 \rangle}}{mc} = \sigma_x \sqrt{\frac{\text{MTE}}{mc^2}} \quad (4)$$

with $\langle p_x^2 \rangle$ the transverse momentum variance, and $\text{MTE} = \langle E_x \rangle + \langle E_y \rangle$ the average transverse kinetic energy of photoemitted electrons, a quantity readily measurable with electron energy analyzers. Here, isotropic photoemission is assumed, i.e., $\text{MTE} = 2\langle E_x \rangle = \langle p_x^2 \rangle / m$. Additionally, for electrons emitted with an excess energy $\langle E \rangle = 3\langle E_x \rangle$ into the vacuum hemisphere, one writes $\text{MTE} = 2\langle E \rangle / 3$. For a given energy gap E_g and positive electron affinity E_a , the simplest model assumes that the photoelectrons are distributed uniformly with kinetic energies between $h\nu - (E_g + E_a)$ and 0, or $\langle E \rangle = [h\nu - (E_g + E_a)] / 2$ and therefore⁵

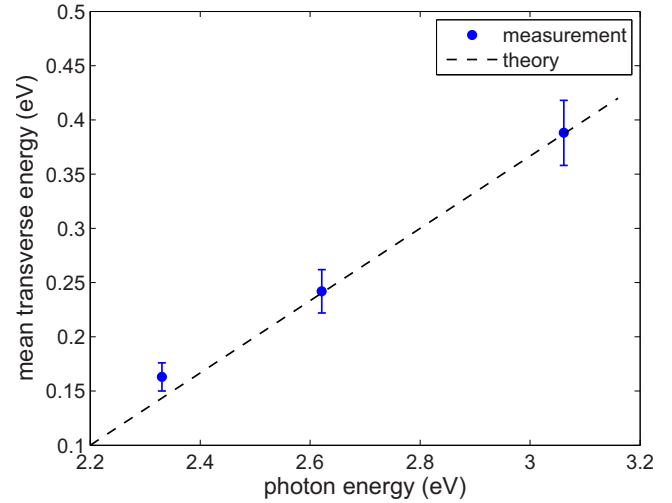


FIG. 5. (Color online) Measured MTE and Eq. (5) vs photon energy.

$$\text{MTE} = \frac{h\nu - (E_g + E_a)}{3} \quad (5)$$

Figure 5 shows MTE obtained from our data and compared with Eq. (5) for energy gap $E_g = 1.2$ eV and electron affinity $E_a = 0.7$ eV.⁶

In summary, the measurements of transverse emittance for CsK₂Sb are presented. The results are found in good agreement with a simple photoemission model. We conclude that this material is very suitable for applications requiring both high QE, low thermal electron emittance, and a prompt response.

This work is supported by NSF (Grant No. DMR-0807731). Two of the authors (S.K. and partially L.C.) are supported by DOE (Grant No. DE-SC0003965).

¹B. M. Dunham, C. K. Sinclair, I. V. Bazarov, Y. Li, X. Liu, and K. W. Smolenski, *Proceedings of the 2007 Particle Accelerator Conference* (IEEE, Albuquerque, 2007), p. 1224.

²L. Cultrera, I. V. Bazarov, J. V. Conway, B. M. Dunham, S. Karkare, Y. Li, X. Liu, J. M. Maxson, and K. W. Smolenski, *Proceedings of the 2011 Particle Accelerator Conference* (IEEE, New York, to be published), WEP244.

³I. V. Bazarov, B. M. Dunham, Y. Li, X. Liu, D. G. Ouzounov, C. K. Sinclair, F. Hannon, and T. Miyajima, *J. Appl. Phys.* **103**, 054901 (2008).

⁴M. P. Stockli, R. F. Welton, and R. Keller, *Rev. Sci. Instrum.* **75**, 1646 (2004).

⁵D. H. Dowell, I. Bazarov, B. Dunham, K. Harkay, C. Hernandez-Garcia, R. Legg, H. Padmore, T. Rao, J. Smedley, and W. Wan, *Nucl. Instrum. Methods Phys. Res. A* **622**, 685 (2010).

⁶C. Ghosh and B. P. Varma, *J. Appl. Phys.* **49**, 4549 (1978).